Linear stability studies in the presence of 3D wall structures

E. Strumberger, P. Merkel, C. Tichmann, and S. Günter

Max-Planck-Institut für Plasmaphysik, EURATOM Association, D-85748 Garching

Introduction: A fusion power plant would require a high beta plasma. However, if neoclassical tearing modes are avoided by a suitable choice of the current profile, external kink modes may limit the achievable plasma beta in tokamak devices. These are ideal modes, growing on a very short time scale of $t \approx 10^{-6}$ s. They could be stabilized by an ideally conducting wall sufficiently close to the plasma boundary. But, in the presence of resistive walls the instabilities grow on a resistive time scale of $t \approx 10^{-3} - 10^{-2}$ s. Since these Resistive Wall Modes (RWMs) grow slowly, their feedback stabilization is technically feasible.

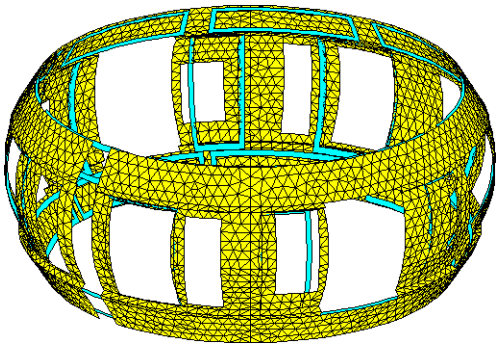

Fig. 1: Resistive wall design (yellow) and feedback coils (cyan) of AUG.

While tokamak plasmas are approximately axisymmetric, realistic external walls may have a complex 3D shape. Figure 1 shows a preliminary resistive wall design for ASDEX Upgrade (AUG) and the 24 feedback coils [1]. The latter are currently being installed in AUG. Breaking the axisymmetry leads to a coupling of the toroidal harmonics, and, as will be shown, to slightly different growth rates depending on the rotational direction of the plasma. Therefore, a 3D numerical treatment of the stability and feedback stabilization studies is necessary.

3D RWM studies: The three-dimensional STARWALL/OPTIM code [2,3] computes growth rates of RWMs and designs robust feedback controllers for their stabilization in the presence of 3D multiply-connected wall structures taking into account coupled toroidal harmonics caused by these 3D walls. Results are presented for an AUG-like test equilibrium, and the 3D, asymmetric wall design shown in Fig. 1.

The plasma equilibrium properties are: major radius $R_0 = 1.64$ m, plasma current $I_p = 0.98$ MA, monotone q-profile with $q_{axis} = 1.46$ and $q_{boundary} = 5.26$, vacuum magnetic field strength $B_0(R_0) = 2.43$ T, and beta normalized $\beta_N = 3.16$. At the low field side the plasma boundary extends to $R \approx 2.14$ m, while the resistive wall is localized at $R \approx 2.23$ m. Therefore, the plasma-wall distance amounts to $\Delta R \approx 9$ cm.

Without wall the plasma is unstable with respect to $n = 1$ (growth rate $\gamma = 48818$ 1/s) and $n = 2$ ($\gamma = 26202$ 1/s) (Higher toroidal mode numbers are not considered in the following studies.), but stable with wall assuming infinite conductivity. In case of a

finite wall conductivity the plasma is unstable on a resistive time scale. Here we used $\sigma d = 2.8 \cdot 10^5$ S with σ being the specific electrical conductivity and d the thickness of the wall.

Figure 2 illustrates the current potential distributions Φ^w [2] in the resistive wall for the pairs of unstable modes. The first two rows show the results obtained for separately computed toroidal harmonics $n = 1$ and $n = 2$. The current pattern clearly reveal the $n = 1$ (first row) and $n = 2$ (second row) mode structure, as well as the phase shift of 90 degrees between the two modes (left and the right coloumn). The growth rates γ of a mode pair are slightly different.

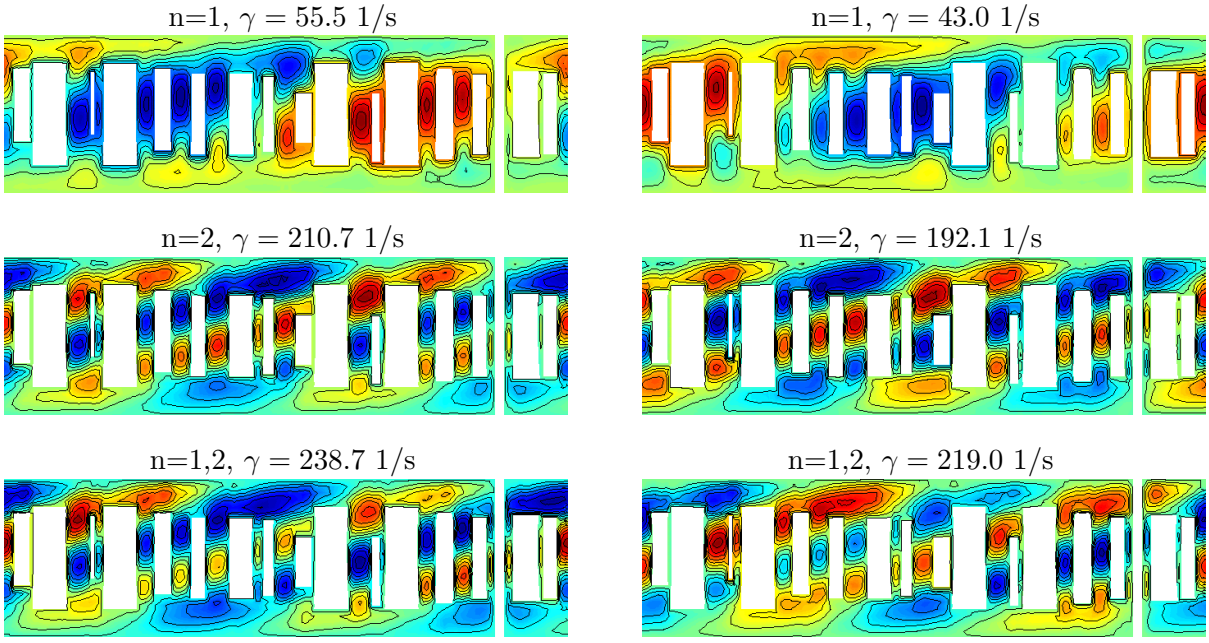

Fig. 2: Current potential distribution Φ^w in the resistive wall for separately computed toroidal harmonics $n = 1$ and $n = 2$ (upper two rows), and coupled harmonics $n = 1, 2$ (last row).

Taking the toroidal harmonics $n = 1$ and $n = 2$ simultaneously into account, one gets 4 unstable modes (γ = 238.7, 219.0, 53.2, and 41.1 1/s). The current distributions of the two most unstable modes are illustrated in the last row of Fig. 2. Not shown are the current pattern of the less unstable modes, because they are similiar to the $n = 1$ pattern presented in the first row. However, the current pattern of the most unstable modes deviate from the corresponding pure $n = 2$ modes, especially the phase shift of the second mode (right column) is changed. This finding is very important for the design of a feedback system. The feedback parameters determined separately for $n = 1$ and $n = 2$ are not able to stabilize the coupled $n = 1, 2$ modes (red dots in Fig. 3), while the feedback parameters determined for the coupled system provide a completely stabilized eigenvalue spectrum (black crosses in Fig. 3).

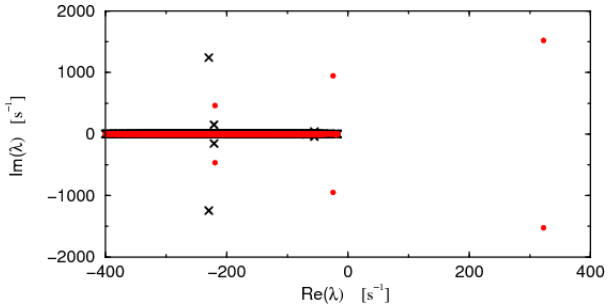

Fig. 3: Eigenvalue spectrum with feedback stabilization.

The 3D STARWALL/OPTIM code is limited to ideal, non-rotating plasma configurations, while realistic tokamak plasmas are resistive, viscous and may rotate in toroidal direction. It is well known that toroidal rotation has an stabilizing effect on RWMs. Since the 2D CASTOR_FlOW code [4] already includes these effects, it was obvious to extend this code to the requirements of a 3D wall geometry, and to combine it with the STARWALL code.

CASTOR_3DW CODE: As the preceding CASTOR versions [4,5] the CASTOR_3DW code uses a Fourier finite-element discretization in the magnetic coordinate system s, ϑ, φ, adopted to the specific axisymmetric equilibrium, with s being the normalized poloidal or toroial flux, and ϑ, φ being the poloidal and toroidal angle coordinates. Because of the 3D wall structure and the resulting coupling of the toroidal harmonics it was necessary to extend the ansatz for the perturbations

$$w_k(s,\vartheta,\varphi) = \sum_{j,p,m,n} \alpha^{k,p}_{m,n,j} h^j_{p,k}(s) \mathrm{e}^{i(m\vartheta+n\varphi)} + \bar{\alpha}^{k,p}_{m,n,j} h^j_{p,k}(s) \mathrm{e}^{-i(m\vartheta+n\varphi)} \qquad (1)$$

by the complex conjugate term (blue) and the sum over the toroidal harmonics n (red). Perturbing the vacuum with unit field perturbations at the plasma boundary, the response of the vacuum is computed with the STARWALL code, and the resulting boundary terms serve as input to the CASTOR_3DW code. This procedure works very well in case of an ideal wall, as demonstrated in Fig. 4 and Table I. There, the CASTOR_3DW results are compared with the results of the 3D ideal CAS3DN code. The latter is a modified version of the CAS3D code [6]. It uses a non-equidistant radial grid, allowing the accumulation of grid points around rational surfaces to obtain the required numerical accuracy.

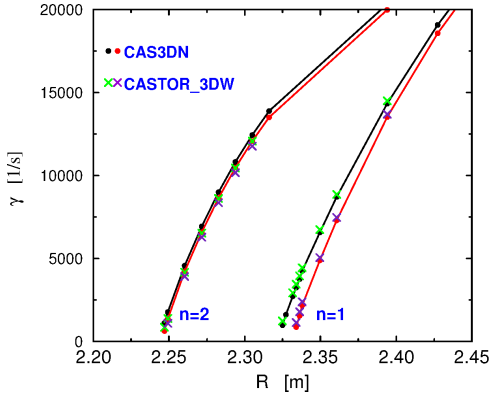

Fig.4: Growth rates of pure $n = 1$ and $n = 2$ modes as function of the ideal wall position.

CASTOR_3DW			CAS3DN		
n=1	n=2	n=1,2	n=1	n=2	n=1,2
32265	24414	32236	32240	24731	32250
31581	24239	31581	31535	24593	31543
		24337			24702
		24241			24573

Table I: Growth rates γ (1/s) of unstable $n = 1$, $n = 2$ and coupled $n = 1, 2$ modes. The 3D ideal wall was localized at $R = 2.56$ m.

Figure 4 shows the growth rates of pure $n = 1$ and $n = 2$ modes as function of the ideal wall distance. The splitting of the growth rates of a toroidal harmonic n increases with decreasing wall distance, because then the small perturbation of the axisymmetry by the 3D wall is effective. Furthermore, the splitting of the growth rates is more pronounced for smaller toroidal harmonics due to the larger radial extension of these modes. The results

listed in Table I verify that the CASTOR_3DW code is also able to determine the growth rates of coupled toroidal harmonics.

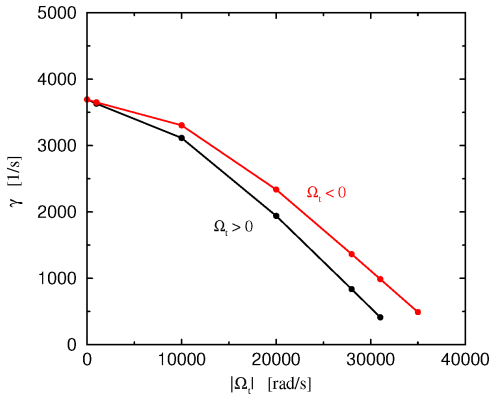

Fig.6: Growth rate as function of the toroidal rotational frequency for $n = 1$.

Figure 6 shows first results obtained with the CASTOR_3DW code taking toroidal plasma rotation into account. For the plasma viscosity we assumed a model for Landau damping [4] with a viscosity coefficient $\kappa_{\|} = 0.89$. As expected, the growth rate descreases with increasing rotational frequency Ω_t. Furthermore, the presence of the 3D wall leads to a dependency of the growth rate on the rotational direction. Again, the effect is more pronounced for smaller growth rates.

The current CASTOR_3DW version in combination with the STARWALL code works very well for an ideal 3D wall. But, in case of a resistive wall the boundary conditions also depend on the eigenvalue. In order to deal with this problem further extensive modifications of the CASTOR_3DW code are necessary.

OUTLOOK: The eigenvalue problem $\lambda \mathbf{Bx} = \mathbf{Ax}$ resulting from the linearized MHD equations [4] (CASTOR_3DW code), and the set of equations [2] derived from the vacuum energy functional (STARWALL code) are coupled by their boundary terms. Combination of these two sets of equations leads to the extended eigenvalue problem

$$\lambda \begin{pmatrix} \mathbf{B}_{ll} & \mathbf{B}_{ls} & \mathbf{0}_{la} \\ \mathbf{B}_{sl} & \mathbf{B}_{ss} & \mathbf{0}_{sa} \\ \mathbf{0}_{al} & \mathbf{0}_{as} & \mathbf{M}_{aa} \end{pmatrix} \begin{pmatrix} \mathbf{x}_l \\ \mathbf{x}_s \\ \mathbf{x}_a \end{pmatrix} = \begin{pmatrix} \mathbf{A}_{ll} & \mathbf{A}_{ls} & \mathbf{0}_{la} \\ \mathbf{A}_{sl} & \mathbf{A}_{ss} & \mathbf{R}_{sa} \\ \mathbf{0}_{al} & \mathbf{R}_{as} & \mathbf{R}_{aa} \end{pmatrix} \begin{pmatrix} \mathbf{x}_l \\ \mathbf{x}_s \\ \mathbf{x}_a \end{pmatrix}. \quad (2)$$

The indices l, s and a refer to the inner part of the plasma, the plasma boundary and the vacuum region, respectively. In order to solve this extended eigenvalue problem, it is necessary to implement some of the STARWALL routines directly into the CASTOR_3DW code. This work is currently in progress.

References:

[1] ASDEX Upgrade Team, IPP, private communication.
[2] P. Merkel et al., 21st IAEA Fus. Ener. Conf., 2006, Chengdu, China, TH/P3-8.
[3] M. Sempf et al., New J. Phys. **11** (2009) 053015.
[4] E. Strumberger et al., Nucl. Fusion **45** (2005) 1156.
[5] W. Kerner et al., J. Comput. Physics **142** (1998) 271.
[6] C. Nührenberg, Phys. Plasmas **3** (1996) 240.